

Mobility-aware Beam Steering in Metasurface-based Programmable Wireless Environments

Christos Liaskos^{*§}, Shuai Nie[†], Ageliki Tsioliaridou^{*}, Andreas Pitsillides[†], Sotiris Ioannidis^{*}, and Ian Akyildiz^{†‡}

^{*}Foundation for Research and Technology - Hellas (FORTH), emails: {cliaskos,atsiolia,sotiris}@ics.forth.gr

[§]University of Ioannina, Computer Science and Engineering Department, Greece

[†]University of Cyprus, Computer Science Department, email: Andreas.Pitsillides@ucy.ac.cy

[‡]Georgia Institute of Technology, School of Electrical and Computer Engineering, emails: {shuainie,ian}@ece.gatech.edu

Abstract—Programmable wireless environments (PWEs) utilize electromagnetic metasurfaces to transform wireless propagation into a software-controlled resource. In this work we study the effects of user device mobility on the efficiency of PWEs. An analytical model is proposed, which describes the potential misalignment between user-emitted waves and the active PWE configuration, and can constitute the basis for studying queuing problems in PWEs. Subsequently, a novel, beam steering approach is proposed which can effectively mitigate the misalignment effects. Ray-tracing-based simulations evaluate the proposed scheme.

Index Terms—Wireless propagation, software-defined, metasurfaces, beam steering, mobility.

I. INTRODUCTION

Software-defined Metasurfaces (SDMs) have received considerable attention, due to their efficiency in exerting control over electromagnetic (EM) waves during their propagation from a transmitter to a receiver [1]. SDMs allow for precise control over the direction, polarization, amplitude and phase of waves impinging over them, in a frequency and encoding-selective manner [2]–[4]. Moreover, metasurface hypervisors called HyperSurfaces (HSFs) have been proposed, which allow for chaining and exerting many wave manipulation functionalities at once via well-defined application programming interfaces [5].

These exquisite capabilities have recently enabled the PWE concept [1]. PWEs are created by applying HSF coating over large planar objects, such as ceilings and walls in floorplans. A central server orchestrates the wave manipulation functions per HSF unit, thereby customizing the wireless propagation *as an app*, tailoring to the locations and needs of the users. Mitigating the NLOS and distance problems in mm-wave communications [6], [7], negating fading phenomena and Doppler Effects, advanced physical-layer security, as well as enabling long-distance wireless power transfer [5] are indicative PWE capabilities.

In order to optimally configure a PWE, the central server needs to sense the wavefronts emitted from the user devices. This task can be handled by the HSFs themselves using embedded sensors [8], or in a sensor-less HSF-synergistic fashion based on compressed sensing principles [9]. In mobility scenarios, however, as shown in Fig. 1, a delay in completing the sense/process/configure cycle may result into

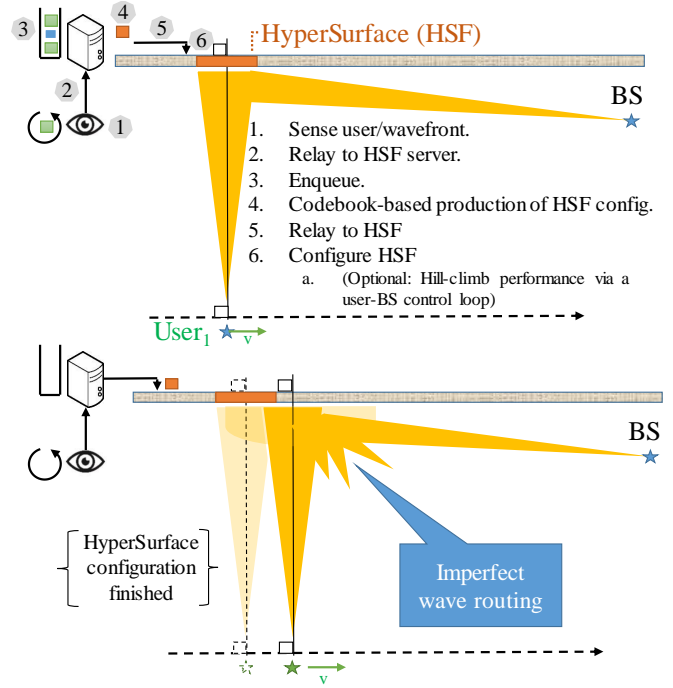


Fig. 1. The considered PWE adaptation cycle, comprising a server that senses the wave emissions from a user and re-configures the HSF accordingly (top). The inserted latency can give rise to misalignment between the user emissions and the HSF configuration (bottom).

misaligned user emissions and HSF configurations, yielding imperfect wave routing.

The contribution of the present study is twofold: first, we model the delay of the HSF sense/reconfigure cycle, accompanied by an analytical approach to study the misaligned beam steering effects. Subsequently, we propose a beam steering configuration that can effectively account for such misalignment, exploiting the high-precision wave manipulation capabilities of SDMs. Ray-tracing-based simulations evaluate the effectiveness of the proposed scheme, also covering cases where some degree of the misalignment phenomenon can be accounted for via user position prediction.

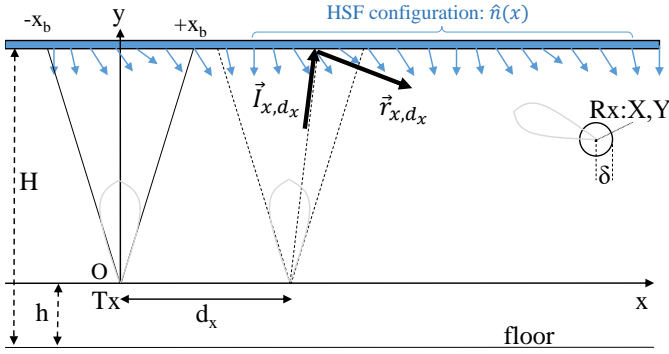


Fig. 2. Illustration of the basic notation employed.

II. SYSTEM MODEL

Consider the setup of Fig. 1 comprising a corridor where the ceiling is HSF-coated, a user moving through it, and a PWE server controlling the HSF configuration adaptively. Ceilings are promising areas to apply HSF coating since they: i) constitute large areas within any floorplan, ii) they are commonly unused, iii) they provide easy access to power supply, and iv) facilitate contact with waves created by user devices such as smartphones: Assuming that the gyroscope of a user device can detect the upwards direction, the user device can subsequently beamform upwards always, meeting the HSF-coated ceiling.

Given the user-emitted wave/HSF contact, the operation of a PWE server follows the steps shown in Fig. 1. First, the HSF impinging wavefront is detected, e.g., by using the HSF-synergistic techniques of [8], [9], or any other external sensory system. Second, this information is relayed in a data packet format to the PWE server via standard networking (e.g., a wired Ethernet link). Third, the information is enqueued at the PWE server, along with the sensory information for all HSF units in the environment, and, fourth, is processed in due time (subject to scheduling). This processing produces the intended configuration of the HSF, via a codebook-based approach [10]. At the fifth step, the sensory information-matching HSF configuration produced is relayed in data packet format to the appropriate HSF unit via standard networking. Finally, at step six, the HSF unit receives this data and changes its state accordingly. The final step may optionally incorporate a HSF configuration hill-climbing sub-step, based on a standard user device-to-BS control loop.

The total duration of this cycle can be expressed as:

$$\tau_{tot} = \tau_s + \tau_n^{\rightarrow} + \tau_q + \tau_p + \tau_n^{\leftarrow} + \tau_c, \quad (1)$$

where τ_s , τ_n^{\rightarrow} , τ_q , τ_p , τ_n^{\leftarrow} and τ_c are the delays attributed to the six steps described above. τ_s can be considered static but technology-dependent (e.g., $10\mu\text{sec}$ for [9], but 10msec for [8]). τ_n^{\rightarrow} and τ_n^{\leftarrow} are generally subject to the networking delay, but may be considered static and equal under the assumption of dedicated and symmetric network paths. τ_q is subject to the scheduling policy of the PWE server, as well as the total sensory load of the PWE network. τ_p can be static and

even negligible in case of codebook-based HSF configuration (e.g., $< 1\mu\text{sec}$ or generally equal to a database lookup query).

In general, the user will have moved by the end of the described cycle. His dislocation, d_x , is a function of τ_{tot} and his mobility pattern, \vec{v} :

$$d_x = f(\tau_{tot}, \vec{v}). \quad (2)$$

We proceed to formulate the possible degradation in the power received by the base station (user uplink) as a function of d_x . We employ the notation of Fig. 2 and consider that $d_x = 0$ at the beginning of step 1 of the PWE server cycle, without loss of generality. The HSF will remain statically configured for $d_x = 0$.

Let \vec{I}_{x,d_x} be the directed power impinging at point x of the HSF, when the user is dislocated by d_x , as shown in Fig. 2, expressed as $\vec{I}_{x,d_x} = P_{x,d_x} \cdot \hat{u}_{x,d_x}$, where:

$$P_{x,d_x} \propto \frac{G_{x,d_x}^{Tx}}{(x-d_x)^2 + (H-h)^2} \cdot \hat{u}_{x,d_x}$$

$$\text{where } \hat{u}_{x,d_x} = \frac{\begin{bmatrix} x-d_x \\ H-h \end{bmatrix}}{\sqrt{(x-d_x)^2 + (H-h)^2}}, \quad (3)$$

G_{x,d_x}^{Tx} being the Tx antenna gain at x . The HSF configuration is generally expressed as a tuple of impinging wave manipulators [5], $\langle \hat{n}, \Delta \vec{J}, \Delta \Phi, a \rangle(x)$, where $\hat{n}(x)$ is a virtually rotated normal at point x of the HSF, defining the reflection of \vec{I}_{x,d_x} as [5]:

$$\vec{r}_{x,d_x} = \vec{I}_{x,d_x} - 2 \left(\vec{I}_{x,d_x} \cdot \hat{n}(x) \right) \hat{n}(x). \quad (4)$$

Moreover, $\Delta \vec{J}(x)$ denotes a rotation of the Jones's vector altering the polarization of \vec{I}_{x,d_x} , while $\Delta \Phi(x)$ and $a(x) \in [0, 1]$ quantify its phase and amplitude alterations by the HSF. We consider an ideal HSF (i.e., with an infinite resolution of meta-atoms), where each component of the HSF configuration tuple can be set and optimized independently¹ and, subsequently focus only on $\hat{n}(x)$. For $d_x = 0$, redirecting $\vec{I}_{x,0}$ to the base station yields the HSF configuration:

$$\hat{n}_*(x) : \exists c > 0 :$$

$$\vec{I}_{x,0} - 2 \left(\vec{I}_{x,0} \cdot \hat{n}_*(x) \right) \hat{n}_*(x) = c \begin{bmatrix} X-x \\ Y-(H-h) \end{bmatrix}, \quad (5)$$

i.e., a reflection that meets the base station location. The total power reaching the base station can then be expressed as:

$$P_{Rx}(d_x) = \int_{-x_b+d_x}^{x_b+d_x} C \left[\vec{I}_{x,d_x} - 2 \left(\vec{I}_{x,d_x} \cdot \hat{n}_*(x) \right) \hat{n}_*(x) \right] G_x^{Tx} dx, \quad (6)$$

where $C[\vec{r}] = \|\vec{r}\|$ if \vec{r} intersects a circle of radius δ positioned at X, Y (as shown in Fig. 2), and 0 otherwise. The x_b limits are employed to capture the main radiation span of

¹In a practical HSFs with limited meta-atom numbers, $\hat{n}, \Delta \vec{J}, \Delta \Phi, a$ may be non-trivially co-joint at x , and also with tuple values in an area around x .

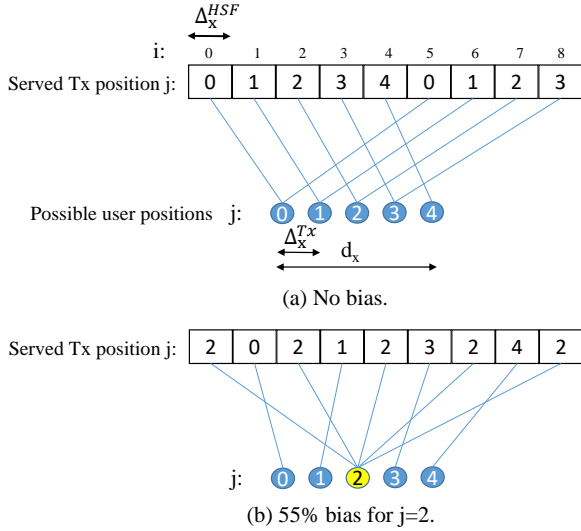


Fig. 3. Visualization of the proposed beam steering approach (a) without bias, and (b) with bias (i.e., a degree of certainty) for a possible user location.

the Tx without loss of generality, and G_r^{Tx} is the base station antenna gain corresponding to \vec{r} . The δ quantity is introduced to capture a non-trivial antenna aperture size at the distance between the reflection point and the base station.

Depending on \hat{n}_* , equation (6) can yield power degradation attributed to the user dislocation d_x . In general, this can be mitigated in three combine-able ways:

- Minimize the networking delay, $\tau_n^{\rightarrow} + \tau_n^{\leftarrow}$, and the queuing delay, τ_q , via appropriate routing and scheduling techniques, thereby minimizing the user dislocation via relation (2).
- Forecast the expected user location at time $t + \tau_{tot}$ and produce the corresponding HSF configuration at step 4 (rather than configuring it for time t).
- Make the HSF configuration aware of the potential user dislocation and mitigate its effects on the received power.

In the next Section we study the latter approach.

III. THE PROPOSED, MOBILITY-AWARE BEAM STEERING

The key-idea behind the proposed beam-steering approach is to exploit the precise wave control offered by the metasurfaces, to cover the full span of the possible Tx positions. This can be accomplished by tuning the HSF configuration, $\hat{n}(x)$, to reflect impinging waves from any probable user location (Tx) to the base station antenna (Rx).

For ease of exposition, we discretize the HSF into sub-units of length Δ_x^{HSF} , over which the \hat{n} configuration remains constant, as shown in Fig. 3. For a HSF of total length L , we index each sub-unit as:

$$i = 0, \dots, I, I = \left\lceil \frac{L}{\Delta_x^{HSF}} \right\rceil. \quad (7)$$

In a similar manner, we discretize the possible user locations with a step of Δ_x^{Tx} , and index them as:

$$j = 0, \dots, J, J = \left\lceil \frac{d_x}{\Delta_x^{Tx}} \right\rceil. \quad (8)$$

Subsequently, let \hat{n}_{ij} be defined as the configuration deployed at sub-unit i of the HSF, steering the reflection from user position j to the base station, i.e., similarly to relation (5):

$$\begin{aligned} \hat{n}_{ij} : \exists c > 0 : \vec{T}_{i, \Delta_x^{HSF}, j, \Delta_x^{Tx}} - 2(\vec{T}_{i, \Delta_x^{HSF}, j, \Delta_x^{Tx}} \cdot \hat{n}_{ij}) \hat{n}_{ij} &= \\ &= c \begin{bmatrix} X - x \\ Y - (H - h) \end{bmatrix}. \end{aligned} \quad (9)$$

Based on the \hat{n}_{ij} definition, we proceed to define a *user position-unbiased HSF configuration beam steering*, illustrated in Fig. 3 (top), as follows:

$$\hat{n}_{ij} : j = \text{mod}(i, J + 1), i = 0 \dots I. \quad (10)$$

The unbiased configuration ensures that at least a portion of the HSF-impinging power will reach the base station. It is intended as a connectivity-ensuring approach, when no further information exists about the location of the user.

We proceed to study the case whether exists an increased confidence for the correct user position, j_c , e.g., expressed as a probability, p_{j_c} , with regard to the other possible positions. In this case, the proposed beam steering becomes *biased* to the outstanding user position. The process is illustrated in Fig. 3 (bottom). First, we set:

$$\hat{n}_{ij_c} : \text{for } i = n \cdot \Delta i, \Delta i = \lceil p \cdot (I + 1) \rceil, n = 0, 1, 2, \dots \quad (11)$$

Then, all i values not covered by relation (11) are set to a j value that follows a round-robin cycle over all possible j values except for j_c .

It is noted that in the biased case, all user positions apart from the outstanding one are inherently assumed to share uniformly the probability of $1 - p$. Producing a configuration that takes into account any probability distribution position over j is a directly applicable generalization, by using techniques from the field of periodic scheduling with multiple concurrent weights [11].

IV. EVALUATION

We evaluate the proposed beam steering approach via ray-tracing based simulations. The employed tool has been presented in [5].

The simulations replicate the setup of Fig. 1, i.e, an open-ended corridor of total height $H = 3\text{m}$ and total length $L = 5\text{m}$. A user device moves at height $h = 1\text{m}$, starting with an offset of $o = 1\text{m}$ from the left side of the corridor. The coordinate system origin is set at this point. The base station is located at $X = 3.6\text{m}$, $Y = 1.4\text{m}$. The user antenna has a beam angle of 30° with uniform, unitary gain and is pointed upwards and in parallel to the y -axis. The base station antenna is similar, but with a beam angle of 60° and oriented towards a counter-clockwise angle of 77° with regard to the y -axis. The system operates at 60 GHz, with the user device (Tx) emitting

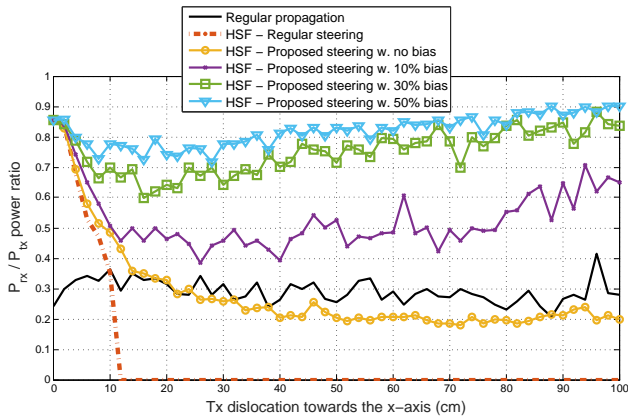


Fig. 4. P_{rx}/P_{tx} ratio of various propagation and beam steering approaches, as the user is displaced towards the x-axis, under static HSF configuration. Notice that the dislocation brings the user physically closer to the base station.

at a power level of 20 dBm and the base station acting as the receiver (Rx).

The HSF-coated ceiling seeks to maximize the P_{rx}/P_{tx} ratio, i.e., ideally directing the totality of the user's emission to the base station. In order to emulate a lossy metasurface, we consider a resolution of $\Delta_x^{HSF} = 1\text{mm}$ across the HSF. In other words, a configured virtual surface normal value is necessarily constant and uniform for Δx . This assumption yields a metasurface of medium efficiency, given that for the studied wavelength $\lambda = 5\text{mm}$, highly efficient metasurface functionality is typically achieved for control at a resolution level of less than $\lambda/10 = 0.5\text{mm}$ [2]. The floor is treated as a perfect conductor and $\Delta_x^{Tx} = 2\text{mm}$.

The HSF is configured correctly for maximizing the P_{rx}/P_{tx} ratio only when the user is located at the coordinate system origin. We are interested in the degradation of the P_{rx}/P_{tx} ratio as the user is displaced towards the x-axis while the HSF configuration remains the same. The regular (non-HSF) propagation is compared to the HSF-enabled propagation under several parameterizations (bias values) of the proposed beam steering.

The results are shown in Fig. 4, with indicative ray-tracing results given in Fig. 5. First, the regular propagation (non-HSF assisted) case yields a P_{rx}/P_{tx} ratio of approximately 30%, given the asymmetry of the Tx-Rx setup and the lack of any natural mechanism for focusing the propagating rays. The efficiency remains almost static during the Tx displacement (noting that this movement reduces the geometric distance of the Tx-Rx pair). All HSF-assisted cases yield an efficiency of 86% when there is no misalignment (Tx dislocation is 0). The 14% loss is due to metasurface losses, as described above.

Second, the HSF-assisted case that employs regular, static beam steering quickly exhibits a drop in its efficiency, which becomes null (i.e., worse than the regular propagation) at a displacement of just 11cm. While such a displacement is significant in mm-wave communications in general, the nullification of the efficiency showcases the necessity for novel

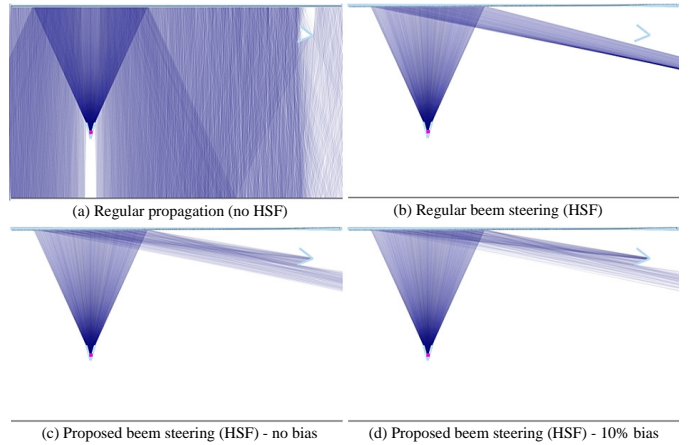


Fig. 5. Ray-tracing based illustrations of the propagation at 20cm Tx dislocation.

beam steering approaches such as the proposed one. Indeed, even with no Tx position bias, the proposed beam steering retains the maximal efficiency of 86% while ensuring near-regular propagation performance in the worst case.

Third, in the case of steering with bias (i.e., guessing the location of the Tx with a very small degree of certainty), even a 10% certainty yields robust performance improvement for any Tx dislocation, which is also significantly better than the regular propagation in any case. At 30% bias, the efficiency is nearly maximized, as exhibited by the fact that subsequently increasing the bias to 50% yields disproportional gains in efficiency. These modest certainty levels could be potentially attained by the vast array of mobility predictors that exist in the literature [12], [13]. Evaluating the synergy between existing predictions and the proposed mobility-aware beam steering algorithm constitutes an open research challenge.

V. CONCLUSION AND OUTLOOK

Software-defined metasurfaces enable precise control over the wireless propagation phenomenon, tailoring it to the needs of users, mitigating distance, fading and mobility effects on wireless communications. The paper studied the effects of misalignment between metasurface configurations and the wireless emissions of the users, which can appear due to latency in the sense/reconfigure cycle of programmable wireless environments. An analytical model was proposed to quantify the misalignment effects, followed by a novel beam steering approach that can mitigate potential misalignment by exploiting the wave manipulation precision offered by metasurfaces.

Further directions can extend the proposed analytical model to a full 3D scenario, while taking into account the complete spectrum of wavefront shaping capabilities offered by metasurfaces. Moreover, the proposed system model can constitute the basis for analyzing misalignment problems from a queuing theory perspective, studying the scheduling problem of sensing and configuring a programmable wireless environment for multiple users. In that aspect, the Age of Information concept can constitute a promising methodological approach [14], [15].

ACKNOWLEDGMENT

This work was funded by the European Union via the Horizon 2020: Future Emerging Topics call (FETOPEN), grant EU736876, project VISORSURF (<http://www.visorsurf.eu>).

REFERENCES

- [1] C. Liaskos, A. Tsioliariidou, A. Pitsillides, S. Ioannidis, and I. F. Akyildiz, "Using any surface to realize a new paradigm for wireless communications," *Communications of the ACM*, vol. 61, pp. 30–33, 2018.
- [2] A. Li *et al.*, "Metasurfaces and their applications," *Nanophotonics*, vol. 7, no. 6, pp. 989–1011, 2018.
- [3] L. Zhang *et al.*, "Space-time-coding digital metasurfaces," *Nature Communications*, vol. 9, no. 1, 2018.
- [4] F. Liu, O. Tsilipakos, A. Ptilakis, A. C. Tasolamprou, M. S. Mirmoosa, N. V. Kantartzis, D.-H. Kwon, M. Kafesaki, C. M. Soukoulis, and S. A. Tretyakov, "Intelligent metasurfaces with continuously tunable local surface impedance for multiple reconfigurable functions," *Physical Review Applied*, vol. 11, no. 4, p. 044024, 2019.
- [5] C. Liaskos, A. Tsioliariidou, S. Nie, A. Pitsillides, S. Ioannidis, and I. F. Akyildiz, "On the network-layer modeling and configuration of programmable wireless environments," *IEEE/ACM Transactions on Networking*, vol. 27, no. 4, pp. 1696–1713, 2019.
- [6] R. Mehrotra *et al.*, "3d channel modeling and characterization for hypersurface empowered indoor environment at 60 ghz millimeter-wave band," in *IEEE SPECTS 2019*, 2019.
- [7] C. Huang, A. Zappone, G. C. Alexandropoulos, M. Debbah, and C. Yuen, "Reconfigurable intelligent surfaces for energy efficiency in wireless communication," *IEEE Transactions on Wireless Communications*, vol. 18, no. 8, pp. 4157–4170, 2019.
- [8] C. Liaskos, G. Pyrialakos, Ptilakis A, S. Abadal, A. Tsioliariidou, A. Tasolamprou, I. F. Akyildiz *et al.*, "Absense: Sensing electromagnetic waves on metasurfaces via ambient compilation of full absorption," in *Proceedings of ACM NANOCOM 2019*.
- [9] C. Liaskos *et al.*, "Joint compressed sensing and manipulation of wireless emissions with intelligent surfaces," in *IEEE DCOSS 2019*, pp. 1–6.
- [10] C. Liaskos, A. Ptilakis *et al.*, "Initial uml definition of the hypersurface compiler middle-ware," *European Commission Project VISORSURF: Accepted Public Deliverable D2.2, 31-Dec-2017*, [Online:] <http://www.visorsurf.eu/m/VISORSURF-D2.2.pdf>.
- [11] C. Liaskos, A. Xeros, G. Papadimitriou, M. Lestas, and A. Pitsillides, "Broadcast Scheduling with multiple concurrent costs," *IEEE Transactions on Broadcasting*, vol. 58, no. 2, pp. 178–186, 2012.
- [12] Ruizhi Wu, Guangchun Luo, Junming Shao, Ling Tian, and Chengzong Peng, "Location prediction on trajectory data: a review," *Big Data Mining and Analytics*, vol. 1, no. 2, pp. 108–127, 2018.
- [13] H. Zhang and L. Dai, "Mobility prediction: A survey on state-of-the-art schemes and future applications," *IEEE Access*, vol. 7, pp. 802–822, 2018.
- [14] I. Kadota, A. Sinha, and E. Modiano, "Optimizing age of information in wireless networks with throughput constraints," in *IEEE INFOCOM 2018 - IEEE Conference on Computer Communications*, pp. 1844–1852.
- [15] M. A. Abd-Elmagid, H. S. Dhillon, and N. Pappas, "A reinforcement learning framework for optimizing age-of-information in rf-powered communication systems," *arXiv preprint arXiv:1908.06367*, 2019.